To cite this version :

Hamid Reza VANAEI, Mohammadali SHIRINBAYAN, Kaddour RAISSI, Sofiane KHELLADI, Abbas TCHARKHTCHI, Michael DELIGANT, Joseph FITOUSSI - A comparative inprocess monitoring of temperature profile in fused filament fabrication - Polymer Engineering & Science - Vol. 61, n°1, p.68-76 - 2020

A comparative in-process monitoring of temperature profile in fused filament fabrication

H.R. Vanaei[1,2] ⓘ | **M. Deligant[1]** | **M. Shirinbayan[2]** ⓘ | **K. Raissi[1]** |
J. Fitoussi[2] | **S. Khelladi[1]** | **A. Tcharkhtchi[2]**

[1]Arts et Metiers Institute of Technology, CNAM, LIFSE, HESAM University, Paris, France

[2]Arts et Metiers Institute of Technology, CNRS, CNAM, PIMM, HESAM University, Paris, France

Correspondence
H.R. Vanaei, Arts et Metiers Institute of Technology, CNAM, LIFSE, HESAM University, F-75013 Paris, France.
Email: hamidreza.vanaei@ensam.eu

Abstract

Fused filament fabrication (FFF), an additive manufacturing technique, is used to produce prototypes and a gradually more important processing route to get final products. Due to the layer-by-layer deposition mechanism involved, bonding between adjacent layers is controlled by the thermal energy of the material being printed. Thus, it is strongly in conjunction with the temperature development of the filaments during the deposition sequence. This study gives out an in-process set-up enabling to record temperature profile of two adjacent filaments or a sequence of deposition in various locations during FFF process. The main characteristic of the presented procedure is the possibility of obtaining a global temperature profile resulted from an IR-camera; parallel to those recorded using a K-type thermocouple. Needless to say that a K-type thermocouple accurately records the local temperature at the interface of adjacent filaments. Conversely, an IR-camera signifies the temperature profile on the captured surface. The obtained results showed that there is a remarkable difference between the cooling rate and re-heating peaks. The primary outcome of this study is the consideration of results accuracy and the possibility of working on optimization of the obtained temperature profile. Altogether it helps optimize inter-layer strength while assessing the temperature evolution.

KEYWORDS
fused filament fabrication, in-process measurement, IR-camera, local-global approach, thermocouple

1 | INTRODUCTION

Fused Filament Fabrication (FFF), an extensively Additive Manufacturing (AM) process,[1] involves extrusion of thermoplastic filaments while moving in successive X-Y planes along the Z direction using the mechanism of layer-by-layer deposition.[2,3]

As deposited filaments are facing with deposition of new filaments during the process, there is always a cyclic temperature profile resulting in the cooling and reheating of each one. The evolution of the temperature profile of filaments during deposition controls the inter-layer bonding. In literature, many works have mentioned the FFF process a thermally driven procedure in which neck growth is stemmed from thermal diffusion of adjacent filaments above the crystallization temperature (for semi-crystalline materials) and the glass transition temperature (for amorphous materials).[4-6]

Variety of studies have been performed to investigate the mechanical strength of 3D-printed parts,[7-10] and it have been pointed out that the evolution of the temperature profile is a key parameter that affects the bonding

quality.[11,12] More specifically, cyclic cooling and re-heating exists during layer deposition of the filaments. The criterion of effective bonding and consequently the mechanical properties are a major concern in FFF.[13,14] In the process of parts fabrication, as the deposition progresses, the hot filament is deposited onto filaments that were previously deposited and/or are being cooled. The contact between the hot filament and the previously deposited filaments causes re-heating of the latter. At the interface of adjacent filaments, temperature rises above the crystallization temperature (T_c) and proper bonding takes place. The evolution of temperature profile could be obtained by employing thermocouples to have local measurements. The deposition; however, might be interrupted while fixing the thermocouple.[15]

Kousiatza et al.[16] locally measured the temperature profile. Although they have had an adequate agreement between experimental and theoretical results, the sudden drop of temperature at the head tip of the extruder showed a gap between the recorded and numerically derived temperature peak values. To wipe out this limitation, infrared thermography has been widely used. Albeit it deals with the surface temperature, it still does not record the interface temperature of adjacent layers.[17] Ferraris et al.[18] used IR thermography in determination of the temperature profile of a vertical wall and they observed poor agreement with theoretical predictions. Furthermore, 1D or 2D models have been developed to evaluate the temperature profile of deposited filaments during fabricating a structure. Sun et al.[5] and Jie Zhang et al.,[19] tried to evaluate, both numerically and experimentally, the influence of process parameters on the temperature evolution. In another study, Bellini and Güçeri[20] used FEM to model extrusion and cooling rate of FFF process. Rodriguez et al.[21] computed the cooling rate numerically as a criterion for the bonding. In addition, Bellehumer et al.[4] developed a 1D model by taking into account the temperature profile. More recently, Costa et al.[22] developed an analytical approach to predict temperature profile and adhesion quality of 3D-printed parts.

For the above-mentioned reasons, experimental monitoring of temperature is still challenging in FFF and lack of practical knowledge corresponds to the problem of bonding in this process. To address this limitation, K-type thermocouples (d = 80 µm) were added in parallel with deposition without pausing the process or causing damage.[23] The experimental data were then compared with the predictions obtained by Costa et al.[24] and it was found that there is a sufficient agreement between the experimental and analytical results.

To conclude, research on in process monitoring of temperature profile is still in its infancy. This work presents a comparison between the local and global assessment of temperature profile using both contact and non-contact approach. The aim is to evaluate the nature of both methods, the IR thermography, and small thermocouples (d = 80 µm) in parallel.

2 | MATERIALS AND METHODS

To track the cooling of filaments and the re-heating peaks of deposition of successive layers during deposition, very small (d = 80 µm) K-type thermocouples were used (see[23] for method description). The schematic of the experiment is presented in Figure 1 containing: the set-up for in-process measurement of temperature profile during the deposition, assembling of two methods together, and thermogram of the printed vertical wall with corresponding layers and locations highlighted for temperature profile. In parallel to the deposition and temperature recording using K-type thermocouples, an Optris PI450 infrared camera was used (at the same points 1-6) with the technical data presented in Table 1. Material emissivity (ε) was obtained by calibrating the absolute difference of the tracks obtained by IR-camera and a thermocouple.

The camera was placed with a specific distance from the extruder to have the plain field of view (FOV) of all the deposited layers. Experiments have been carried out while the camera inspecting (a) the X-Z planes and (b) the Y-Z planes. In the first case (X-Z planes), the printed part is stationary on FOV. It was then recorded temporal temperature variations in the object front plane. Therefore, temperature changes at every location are the consequence of several re-heating that stem from new depositions. In-process monitoring was performed on a designed vertical wall sample with geometry of 50×0.2×35 mm^3 using the one-way direction of deposition. Process parameters and related settings to the process are indicated in Table 2.

In the second case (Y-Z planes), the nozzle was fixed and the part was printed by moving the built plate in Y direction. Four points specified as shown in Figure 2 with the following descriptions. Point a stays on extruder during printing (verifying the extruder temperature and the accuracy of measurement). Point b specifies the variation of temperature when material exits from the extruder (diffusion zone of material between two adjacent layers). Point c indicates the temperature of same layer. In other word, it is located on the same layer as that of point b, but with a specific distance from extruder (out of diffusion zone). Point d represents the effect of extruder temperature (or material when exits from extruder) on the previous layer (end of diffusion zone).

Temperature difference (ΔT) between point b and d is an indicator of temperature profile between two
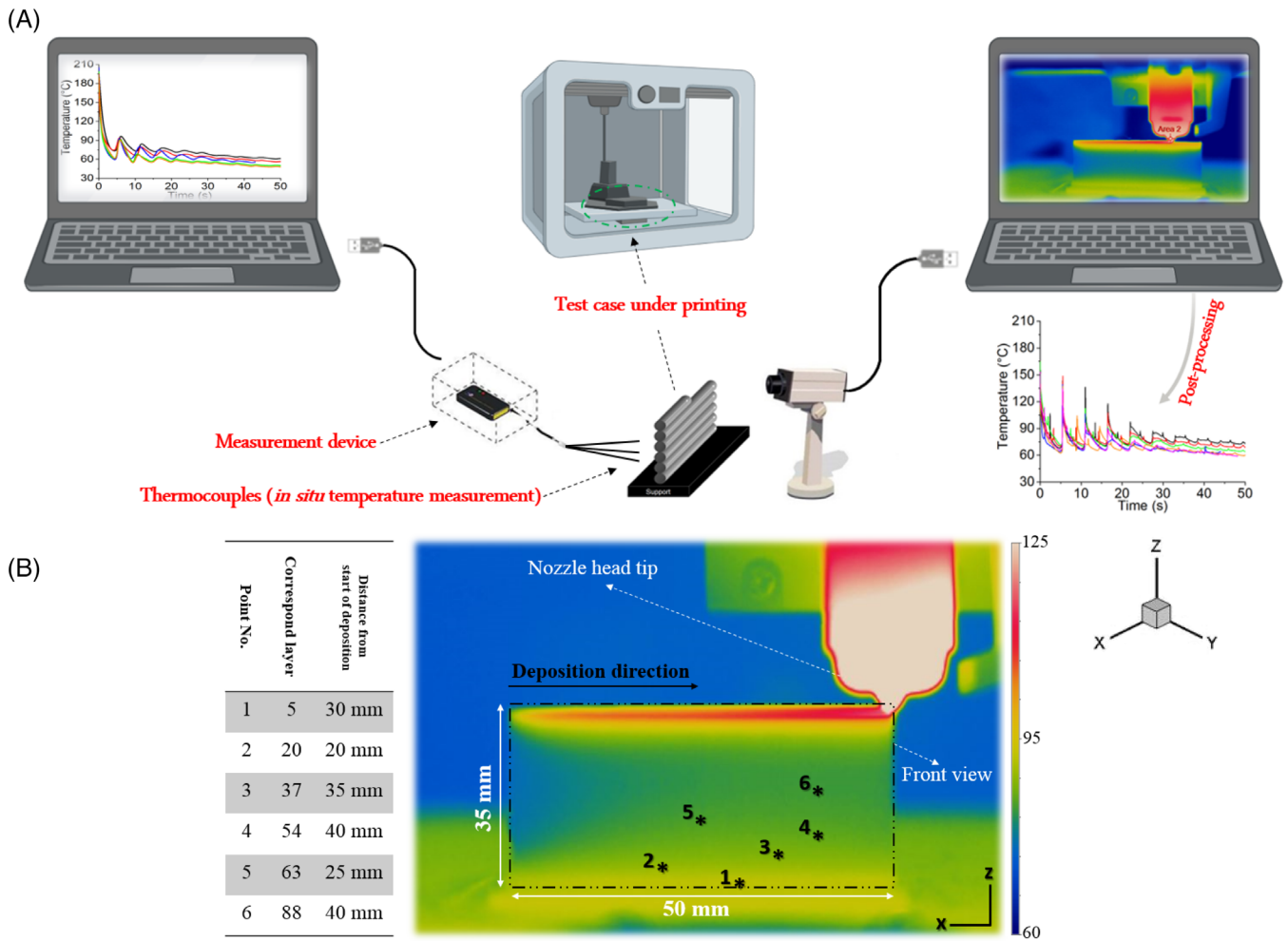
FIGURE 1 Representation of (A) in situ measurement of temperature profile during the deposition stage in FFF process, (B) thermogram of a vertical wall and points representing the location of the thermocouples with corresponding layers highlighted for temperature profile [Color figure can be viewed at wileyonlinelibrary.com]

TABLE 1 Technical data of Optris PI 450 camera

Technical data	Value
Wavelength range (μm)	8-14
Frequency (Hz)	32
Frame rate (Hz)	80
Optical resolution (pixels)	382*288
Material emissivity	0.89
Accuracy (%)	±2

TABLE 2 Process parameters used for printing

Parameter	Value
Liquefier temperature (°C)	210
Support temperature (°C)	50
Printing speed (mm/s)	20
Layer height (mm)	0.2
Infill (%)	100

adjacent layers. It could be compared with point c for complementary assessment of the inter-layer temperature evolution. Two cases have been shown as (a) deposition from first layer-to-layer 5 and (b) deposition from layer 15 to layer 20 to show the influence of distance from the heat flux of support.

To perform the experimental procedure, polylactic acid (PLA) filament (d = 1.75 ± 0.01 mm) with the density of $\rho = 1.24$ g/cm^3 has been used (fillamentum supplier). Differential scanning calorimetry (DSC) was done using DSC Q1000 from TA instrument. Sample ($\sim$6 mg), cut from the printed part, was sealed in an aluminum pan and heated from room temperature to 200°C with heating rate of 5°C/min to determine crystallization and melting temperature, T_c and T_m, respectively. The related curve and the gathered data are presented in Table 3. The temperature range between $T_c = 103$°C and $T_m = 148$°C is an important temperature range in the FFF process in semi-crystalline materials.
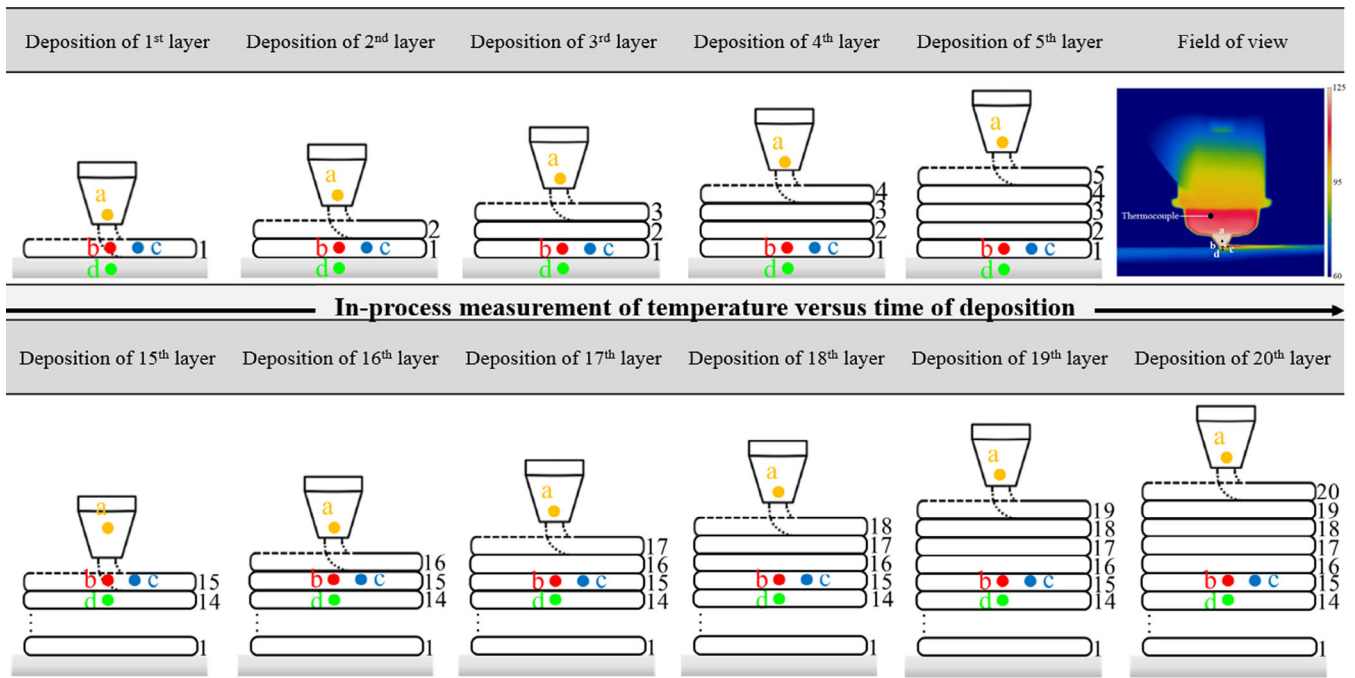
FIGURE 2 Schematic representation of temperature variation of point a-d at instance of deposition for (A) layer 1 to 5 and (B) layer 15 to 20 [Color figure can be viewed at wileyonlinelibrary.com]

TABLE 3 Differential scanning calorimetry curve and thermal properties of PLA

DSC curve	Properties	PLA material
	T_c (°C)	103
	T_m (°C)	148

3 | RESULTS AND DISCUSSION

3.1 | Local and global temperature profile

The accompanying graphs presented in Figure 3 provide the experimental results (temperature profile) of both IR-camera and K-type thermocouple. They comprise six points in different locations (in different layers) of the sample (see Figure 1). As described, the reported experiments are based on the layer-by-layer deposition of filaments. Under the 3D printing conditions, when a new filament is deposited, the previous one has significantly cooled down. Although there is a notable variance in starting point (when the filament exists from the nozzle) of deposition for each layer, the temperature evolves in the same cooling rate. For post processing, the two signals are synchronized at $t = 0$, based on the instant of the first peak of temperature (the highest measured value considered as a value at $t = 0$).

As illustrated in Figure 4, the temperature peaks recorded by both methods is described as following. Peak 1 is the re-heating of fifth filament by deposition of sixth filament; peak 2 is the re-heating of fifth filament by deposition of seventh filament; peak 3 is the re-heating of fifth filament by deposition of eighth filament; peak 4 is the re-heating of fifth filament by deposition of ninth filament. Peaks on cooling curves are the return of the extruder to the point of next deposition without feeding of material (not important).

Owing to the nature of thermocouple and the local measurement of temperature at the inter-layer bonding, the temperature peaks recorded by IR-camera are highly overestimated comparing with those recorded by the K-type thermocouple. On the other hand, the sequences of temperature peaks concluded by K-type thermocouple has an acceptable evolution in comparison with those derived from IR-camera. In almost all the conditions, by increasing the distance
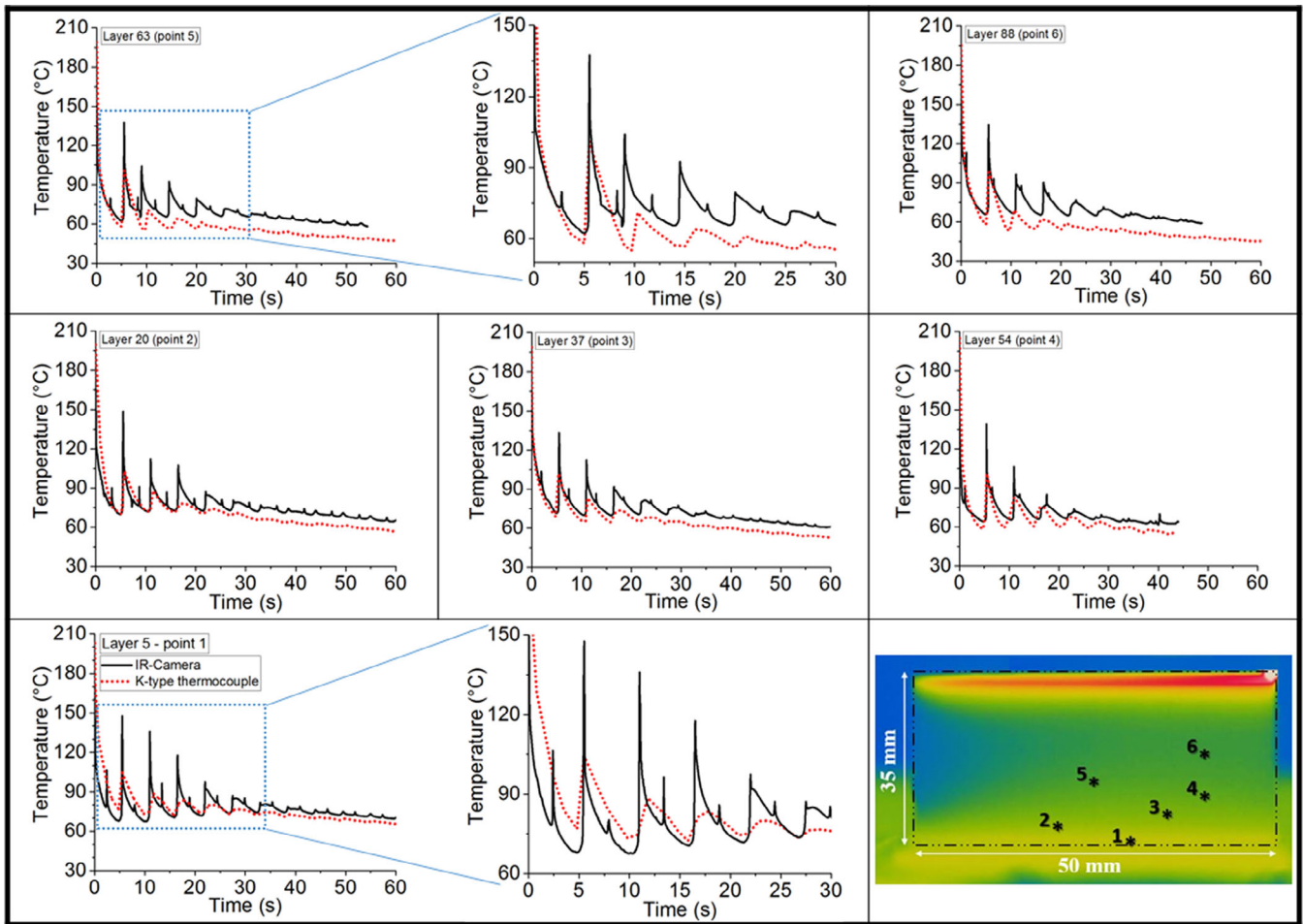
FIGURE 3 Temperature evolution at six locations during the deposition of a vertical wall consisting of single filaments deposited on top of each other. Point 1–6 corresponds to the fifth, 20th, 37th, 54th, 63rd, and 88th while indicating 30, 20, 35, 40, 25, and 40 mm from start of deposition, respectively [Color figure can be viewed at wileyonlinelibrary.com]
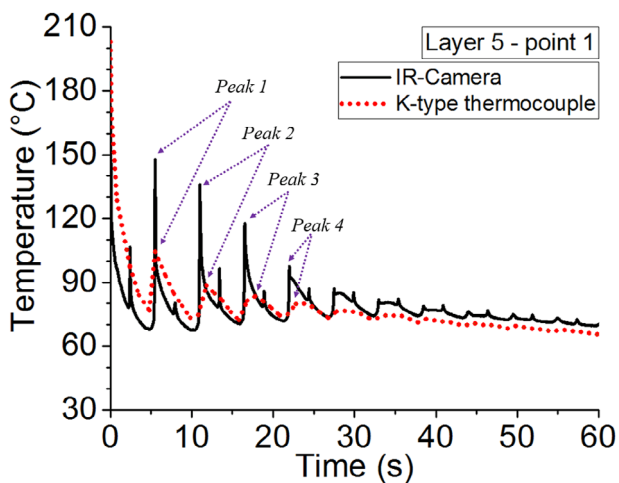

FIGURE 4 Experimental temperature evolution of layer 5 (at x = 30 mm) during the deposition of a vertical wall consisting of single filaments deposited on top of each other [Color figure can be viewed at wileyonlinelibrary.com]

from the support, the temperature profile remains above 50°C. The secondary re-heating (and consequently third, fourth, fifth, and other re-heatings) are increasingly weak enough to enhance and keep the temperature of the previously printed parts. Accordingly, the inter-layer diffusion is limited to adjacent filaments as the secondary re-heating peak is at almost T = 103 (±2)°C.

Presented results in Figure 3 showed that there is a notable difference between the monitored temperature profiles. Despite the acceptable precision of the IR-camera, peak values (particularly in the first 20 seconds) are overestimated. This could be deduced from the radiation of extruder, previously deposited filaments under cooling, or even the heat radiation from support for the first layers. Believably, the precision of the IR-camera is lower than a thermocouple based on the nature of each measurement method. It has some

advantages such as straightforwardness of the test and overfilling of data. In future work, numerical validation of both methods will be done for further discussions.

FIGURE 5 Upper-limit and peaks evolution of data recorded at each layer by (A) IR-camera and (B) type K thermocouple [Color figure can be viewed at wileyonlinelibrary.com]

3.2 | Upper-limit and peaks evolution

Re-heating peaks decrease with progressively deposition of filaments. As mentioned in section 2, the temperature above T_c and below T_m is important for inter-diffusion of successive layers. Cyclic evolution of temperature plays an important role in the overall incident. In Figure 5, upper-limit of peak consequences indicates two different observations. Seemingly, the first data recorded by the IR-camera (refer to Figure 5(A) decreases about 23% with a distance increase from support, whereas, those captured by the K-type thermocouple (refer to Figure 5(B) stay around 5%. Apparently, on behalf of the extruder temperature, the thermocouple hands over ∼4% deviation from real data ($T_{ext} = 210°C$) while ∼19% by the IR-camera. As an example, the first data recorded by K-type thermocouple and IR-camera for layer 54 at x = 40 mm from deposition are 202°C and 155°C, respectively.
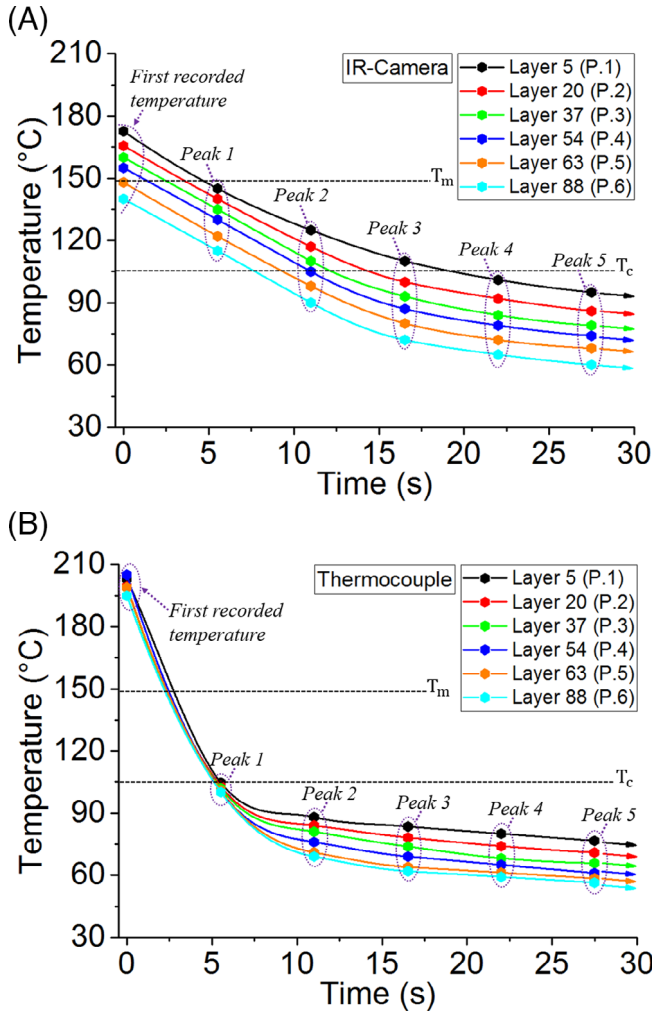
3.3 | Interval of peaks between two approaches

Following observations obtained so far: layers near support are more affected by T_{supp} (higher peaks in IR-camera); layers in the middle distance are less affected by T_{supp}. Whereas T_{supp} does not affect layers far from the support (Recorded peaks by IR-camera are near those recorded by thermocouple).

Table 4 shows the "$\Delta T = T_{IR-camera} - T_{thermocouple}$" at each peak. Worth mentioning that based on described features, such as, support radiation, there is a small difference in correspond peaks at layers far from the support.

The graphs in Figure 6 reveal the difference of upper-limit obtained by both methods as a function of building time. The specified contour for each layer expresses the nature of each measurement method. Apparently, temperature varies between T_c and T_m in first layers, whereas, the contour drops below T_c as the

	IR-camera and thermocouple temperature difference at each peak (°C)				
Layer	**1**	**2**	**3**	**4**	**5**
5	44.9	31.5	34.2	21	18.4
20	43	29	26.8	18	15.1
37	37.3	27	21.2	15.8	13.2
54	36.5	25.3	13.7	12.1	9.9
63	33.5	24.3	11.1	10.8	9.6
88	33.2	21	8.1	5.8	3.6

TABLE 4 Data collected from the difference in peak values (Calculated using "$\Delta T = T_{IR-camera} - T_{thermocouple}$" at each peak)
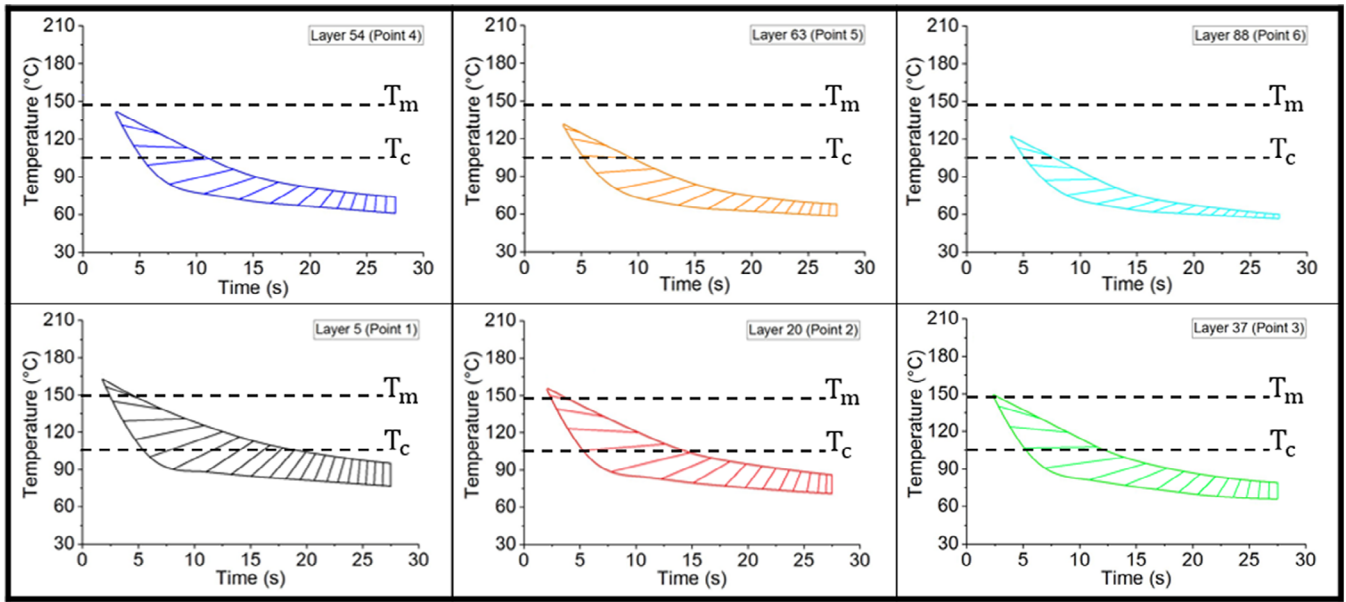
FIGURE 6 Temperature contour at six locations during the deposition of a vertical wall consisting of single filaments deposited on top of each other. Point 1-6 corresponds to the fifth, 20th, 37th, 54th, 63rd, and 88th while indicating 30, 20, 35, 40, 25, and 40 mm from start of deposition, respectively [Color figure can be viewed at wileyonlinelibrary.com]
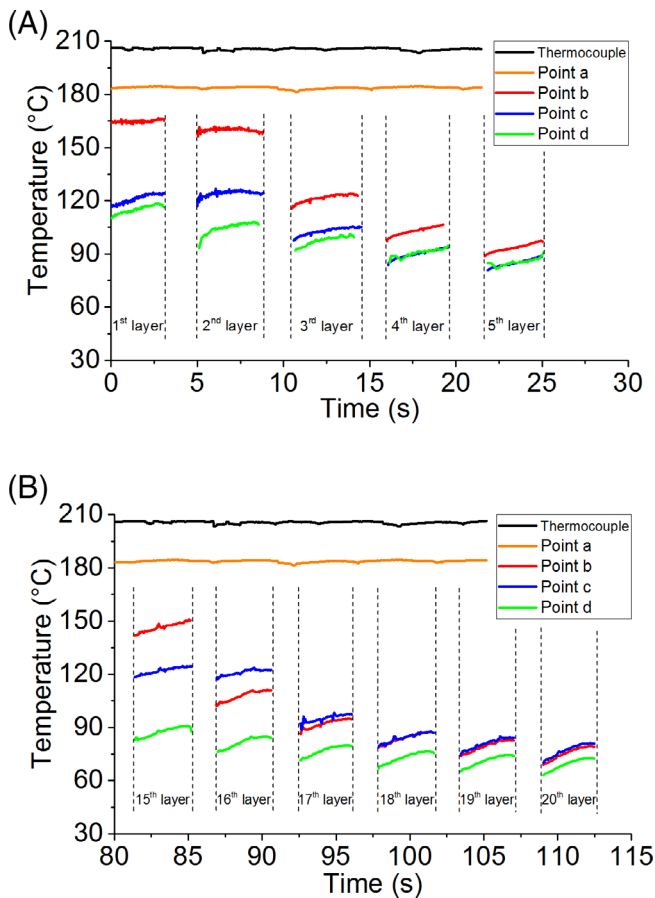

FIGURE 7 Temperature variation of point a-d at instance of deposition for (A) layer 1 to 5 and (B) layer 15 to 20 [Color figure can be viewed at wileyonlinelibrary.com]

distance from the support is increasing. Their relative change is an important concern in the problem of inter-layers bonding and it should be taken into consideration.

3.4 | Four points on IR-camera (second experiment with stationary nozzle)

To have better comprehension, four points have been chosen around the extruder based on Figure 2 (in section 2). The temperature was recorded with the deposition. The mechanism of recording could be explained: the location of points a-d are fixed while the support is moving and it means that at any instance of deposition, the temperature variation of each point is recording. This partially clarifies the temperature of points a-d from beginning of the deposition of a layer and progressively the successive layers.

Figure 7 shows the obtained results. They cover the previous assumptions displaying the effect of distance from support. Presumably from Figure 7(A) and by deposition from layer one to layer five, the temperature of point b shifts between 165°C and 90°C. This is also valid for point c while temperature shifts between 120°C and 80°C. Figure 7(B) could explain the general statement by observing the evolution of point b shifts from 150°C and 70°C by progressive deposition of further layers. In fact, one can note that after a specific deposition of layers (in this case after layer 15) points b and c have almost the

TABLE 5 Strengths and limitations of approaches introduced in this study

Approach	Strengths	Limitations
K-type thermocouple (Local approach)	In situ Temperature profile at interface of adjacent filaments Using obtained results in bonding studying Using obtained results in neck-growth and welding of filaments	Incapable of temperature recording in complex geometry
IR-camera (Global approach)	In situ Capable of temperature recording in complex geometry	Temperature profile on surface of adjacent filaments Incapable of recording temperature of adjacent filaments Over-estimation of recorded peaks Sudden drop of the recorded value

same temperature. Worth mentioning to say, point d remains constant after third layer. For instance, the distance across point b and d during deposition of the first layer expresses the inter-layer diffusion zone. It varies from 165°C to 100°C that is approximately between T_c and T_m. This issue thoroughly explains the cyclic temperature profile discussed before.

3.5 | Comparison of two applied approaches

A vertical wall of a single filament thickness is considered for the analysis of thermal interaction by employing two methods: IR-camera as a global and applying K-type thermocouples as a local approach. As can be seen from the obtained results and depending on the nature of measurement methods, both local and global in-process monitoring of temperature profile have their own strengths and limitations (see Table 5).

As listed in Table 5, regarding the nature of measurement approach and the obtained experimental results, one can note that the capability of each approach as well as their strengths and limitations has a determinative role in the evaluation of temperature profile. Nevertheless, an entire optimization between two approaches could precisely result in characterization of thermal behavior during fabrication of 3D printed parts.

4 | CONCLUSIONS AND PERSPECTIVES

This work presents an in-process set-up enabling the record of temperature profile of two adjacent filaments

(and/or a sequence of deposition) in various locations during the FFF process. The main characteristic of the presented procedure is the possibility of obtaining a global temperature profile resulted from the IR-camera; parallel to those recorded using a K-type thermocouple (local temperature at interface). Accurate acquisition via local measurement revealed by putting K-type thermocouples in different successive layers. However, IR-camera showed that there is a considerable difference by increasing the distance from support. A comparison through the upper-limit and interval of peaks validated the mentioned difference. The obtained experimental results showed that the optimization of the results obtained with the IR-camera by those achieved using the K-type thermocouples are necessary for the bonding optimization.

Additional experiments with a numerical validation are necessary to the set-up and its usefulness. Future work will focus on applying the results in complex geometry with a controlled-environment (Chamber) temperature and developing a predictive approach. This study is useful in inter-layer bonding optimization of adjacent layers by implementing the temperature evolution of filaments.

ORCID

H.R. Vanaei https://orcid.org/0000-0003-1501-0482
M. Shirinbayan https://orcid.org/0000-0002-2757-8529

REFERENCES

[1] J. Holmström, J. Partanen, J. Tuomi, M. Walter, *J. Manuf. Technol. Manage.* **2010**, *21*(6), 687.

[2] P. Chennakesava, Y. S. Narayan, Fused deposition modeling-insights. in *Proceedings of the International Conference on Advances in Design and Manufacturing ICAD&M*, Vol. 14 **2014**, p. 1345.

[3] T. Ambone, A. Torris, K. Shanmuganathan, *Polym. Eng. Sci.*

[4] C. Bellehumeur, L. Li, Q. Sun, P. Gu, *J. Manuf. Processes* **2004**, *6*(2), 170.

[5] Q. Sun, G. Rizvi, C. Bellehumeur, P. Gu, *Rapid Prototyping J.* **2008**, *14*(2), 72.

[6] A. K. Ravi, A. Deshpande, K. H. Hsu, *J. Manuf. Processes* **2016**, *24*, 179.

[7] W. Wu, P. Geng, G. Li, D. Zhao, H. Zhang, J. Zhao, *Materials* **2015**, *8*(9), 5834.

[8] R. Zaldivar, D. Witkin, T. McLouth, D. Patel, K. Schmitt, J. Nokes, *Addit. Manuf.* **2017**, *13*, 71.

[9] H. R. Vanaei, M. Shirinbayan, M. Deligant, K. Raissi, J. Fitoussi, S. Khelladi, A. Tcharkhtchi, *Polym. Eng. Sci.* **2020**, *60*, 1822. https://doi.org/10.1002/pen.25419.

[10] B. Huang, S. Meng, H. He, Y. Jia, Y. Xu, H. Huang, *Polym. Eng. Sci.* **2019**, *59*(1), 120.

[11] A. D'Amico, A. M. Peterson, *Addit. Manuf.* **2018**, *21*, 422.

[12] H. R. Vanaei, K. Raissi, M. Deligant, M. Shirinbayan, J. Fitoussi, S. Khelladi, A. Tcharkhtchi, *J. Mater. Sci.* **2020**, *55* (29), 14677. https://doi.org/10.1007/s10853-020-05057-9.

[13] E. Brandl, U. Heckenberger, V. Holzinger, D. Buchbinder, *Mater. Des.* **2012**, *34*, 159.

[14] F. Wang, *Int. J. of Adv. Manuf. Technol.* **2012**, *58*(5–8), 545.

[15] C. Kousiatza, D. Karalekas, *Mater. Des.* **2016**, *97*, 400.

[16] C. Kousiatza, N. Chatzidai, D. Karalekas, *Sensors* **2017**, *17*(3), 456.

[17] J. E. Seppala, K. D. Migler, *Addit. Manuf.* **2016**, *12*, 71.

[18] E. Ferraris, J. Zhang, B. Van Hooreweder, *CIRP Annals* **2019**, *68*, 213.

[19] J. Zhang, X. Z. Wang, W. W. Yu, Y. H. Deng, *Mater. Des.* **2017**, *130*, 59.

[20] A. Bellini, S. Güçeri, *Rapid Prototyping J.* **2003**, *9*, 252.

[21] J. F, M. A. T. A. S. RODRIGUEZ, J. P. Thomas, J. E. Renaud, *J. Mech. Des.* **2003**.

[22] S. Costa, F. Duarte, J. Covas, *J. Mater. Process. Technol.* **2017**, *245*, 167.

[23] H. R. Vanaei, M. Shirinbayan, S. F. Costa, F. M. Duarte, J. A. Covas, M. Deligant, S. Khelladi, A. Tcharkhtchi, *J. Appl. Polym. Sci.* **2020**, 1. https://doi.org/10.1002/app.49747.

[24] S. Costa, F. Duarte, J. Covas, *Virtual Phys. Prototyping* **2015**, *10* (1), 35.